Materials Today Communications 35 (2023) 105671

Contents lists available at ScienceDirect

Materials Today Communications

journal homepage: www.elsevier.com/locate/mtcomm

Oxidative ethanol dry reforming for production of syngas over Co-based catalyst: Effect of reaction temperature

Fahim Fayaz [a,b,*], Chao He [b], Avishek Goel [b], Jukka Rintala [b], Jukka Konttinen [b]

[a] Faculty of Chemical and Process Engineering Technology, Universiti Malaysia Pahang, Lebuhraya Tun Razak, 26300, Gambang, Kuantan, Pahang, Malaysia
[b] Faculty of Engineering and Natural Sciences, Tampere University, Korkeakoulunkatu 8, 33720 Tampere, Finland

ARTICLE INFO

Keywords:
Oxidative ethanol dry reforming
Hydrogen
Syngas
Cobalt

ABSTRACT

Till date, oxidative ethanol steam reforming use Ni-based catalysts to produce syngas. However, Ni catalysts suffer from easy deactivation due to the coke formation at low temperatures. Therefore, oxidative ethanol dry reforming is a promising method and was investigated over 10 %Co/Al_2O_3 catalyst due to their high activity and stability to produce high-quality syngas. More importantly, the syngas can be upgraded to produce liquid biofuels and chemicals. The catalyst was evaluated in a quartz fixed-bed reactor under atmospheric pressure at $P_{CO_2} = P_{O_2} =$ 5 kPa, $P_{C_2H_5OH} =$ 15 kPa, with reaction temperature ranging between 773 and 973 K. The γ-Al_2O_3 support and 10 %Co/Al_2O_3 catalyst had BET surface areas of 175.^{2} m^2 g^{-1} and 143.1 m^2 g^{-1}, respectively. Co_3O_4 and spinel $CoAl_2O_4$ phases were detected through X-ray diffraction measurements on the 10 %Co/Al_2O_3 catalyst surface. H_2-TPR measurements indicate that the 10 %Co/Al_2O_3 catalyst was completely reduced at a temperature beyond 1000 K. NH_3-TPD measurements indicated the presence of the weak, medium, and strong acid sites on the γ-Al_2O_3 support and 10 %Co/Al_2O_3 catalyst. Due to increased reaction temperature from 773 to 973 K, C_2H_5OH and CO_2 conversions improved from 22.5 % to 93.6 % and 16.9–52.8 %, respectively. Additionally, the optimal yield of H_2 and CO obtained at 68.1 % and 58.3 %, respectively. Temperature-programmed oxidation experiments indicated that the amount of carbon deposition was the lowest (28,92 %) at 973 K and increased by 41.48 % at 773 K.

1. Introduction

The increase in crude oil prices and its negative impact on the environment such as air pollution, ozone depletion, and climate change has led to the growing interest in the use of renewable and less-pollutant resources [1,2]. Synthetic gas (or syngas), a mixture of CO and H_2 is recognized as an environmentally friendly alternative energy source in recent years and it can be directly used as a fuel source for electricity generation and transport fuel [3,4]. Commonly, syngas is produced through partial oxidation of methane [5], methane steam or dry reforming [6,7], oxidative methane steam or dry reforming [8,9], ethanol steam or dry reforming [10,11] and oxidative ethanol steam reforming [12]. However, methane from natural gas is not a renewable source and thus its availability is limited. There is a growing interest in the use of ethanol among biomass-derived feedstocks [13]. Compared to other feedstocks such as, glycerol, ethanol offers low toxicity, ease of production in large quantities, relatively high hydrogen content and it is free from sulfur-containing compounds [14]. Ethanol can be produced either by fermenting sugar or starch (first generation) or hydrolysing lignocellulose and fermenting it (second generation) [15]. There have been many studies conducted on reforming processes using both non-noble (Ni-based catalysts) and noble metal (Pt and Rh) catalysts to produce syngas. Osaze et al. studied the effect of temperature from 923 to 1023 K over 10 %Ni/SBA-15 catalyst on the performance of methane dry reforming and found that when temperature increased both CH_4 and CO_2 conversions raised about 83.4 % and 59 %, respectively due to endothermic nature of methane dry reforming [16]. However, Ni catalysts are currently faced with the challenge of early deactivation caused by the coke formation at lower temperatures [17]. In addition, cobalt-based catalysts are also used to produce syngas from oxidative ethanol steam reforming due to their high activity, stability, and low-cost alternative to noble metals [18,19]. Pereira et al. investigated the catalytic behavior and regeneration processes of oxidative ethanol steam reforming over Co/SiO_2, Co–Rh/SiO_2, and Co–Ru/SiO_2 catalysts.

* Corresponding author at: Faculty of Chemical and Process Engineering Technology, Universiti Malaysia Pahang, Lebuhraya Tun Razak, 26300, Gambang, Kuantan, Pahang, Malaysia.
E-mail address: fahim.fayaz@tuni.fi (F. Fayaz).

https://doi.org/10.1016/j.mtcomm.2023.105671
Received 23 October 2022; Received in revised form 29 January 2023; Accepted 17 February 2023
Available online 18 February 2023

By using oxidative treatment, $CoRh/SiO_2$ and $CoRu/SiO_2$ catalysts were activated, resulting in higher ethanol conversion and hydrogen selectivity after regeneration [20]. Sukri et al. also studied the effect of cobalt loading (Co=10 %, 15 %, 20 % and 25 %) over Co/MgO catalysts in methane dry reforming and found that the 10 %Co catalyst showed good activity, stability, the highest CH_4 and CO_2 conversions, and the lowest rate of carbon deposition at 750 °C [21]. Thus, a new, and environmentally more positive approach is oxidative ethanol dry reforming (OEDR) (cf. Eq. (1)), which converts CO_2 greenhouse gas and produces value-added synthesis gas.

$$3C_2H_5OH + CO_2 + O_2 \rightarrow 7CO + 9H_2 \left(\Delta H^0_{298K} = 325.3 kJmol^{-1}\right) \quad (1)$$

To the best of our knowledge, none of the available studies have explored oxidative ethanol dry reforming over Co/Al_2O_3 catalyst. Therefore, the objective of this was the chemical and physical characteristics of 10 %Co/Al_2O_3 catalyst in addition to investigating the effect of reaction temperature on the activity and selectivity of OEDR reaction.

2. Experimental

2.1. Synthesis of catalyst

The wet impregnation method was used to impregnate 10 % (by weight, metallic) cobalt on alumina [21]. To ensure thermal stability, an adequate amount of puralox alumina (SCCa-150/200 procured from Sasol, Hamburg, Germany) was calcined for 5 h at 1023 K in a Carbolite (Bemaford, Sheffield, UK) furnace with air and a heating rate of 5 K min^{-1}. An aqueous solution of $Co(NO_3)_3.6\ H_2O$ was supplied and magnetically stirred for 3 h with pretreated γ-Al_2O_3 support in am ambient environment (Sigma- Aldrich, St. Louis, Missouri). The mixture was dried at 383 K for 24 h. Moreover, it was calcined in air with a heating rate of 5 K min^{-1} and kept at constant temperature of 773 K for 5 h. Post crushing and sieving, the catalyst was introduced into a fixed-bed reactor with a particle size between 125 and 160 μm.

2.2. Characterization of catalyst

Micromeritics ASAP-2020 (Norcross, Georgia) at 77 K was used to measure Brunauer-Emmett-Teller (BET) surface areas for 10 %Co/Al_2O_3 catalyst and γ-Al_2O_3 support. During BET measurement, the example was degassed for 1 h at 573 K in N_2 flow to remove moisture and volatile contaminants. Rigaku Miniflex II (Akishima-shi, Tokyo, Japan) X-ray diffraction system was utilized to study the crystal structure of γ-Al_2O_3 support and 10 %Co/Al_2O_3 catalyst at 30 kV and 15 mA and Cu target was used as a source of radiation (wavelength, λ of 1.5418 Å). Diffraction patterns were scanned from 3° to 80° with an imaging speed of 1° min^{-1} and a step size of 0.02° to obtain high-resolution X-ray diffractograms. A software tool (Match! version 2.3.3) was used to measure all X-ray patterns. A micromeritics AutoChem II-2920 apparatus was used for both alumina and 10 %Co/Al_2O_3 catalyst to conduct the H_2-TPR experiment. The U-tube of quartz was loaded with 0.1 g of sample and sandwiched with quartz wool. As an initial treatment, the sample was heated to 373 K under 50 ml min^{-1} in He flow for 30 min to remove volatile compounds from the sample. Following this, the temperature of the sample was increased to 1173 K and kept at the constant temperature for 30 min under 50 ml min^{-1} 10 %H_2/Ar mixture. The amount of carbon accumulated on the spent specimen surface after OEDR, temperature-programmed oxidation (TPO) was measured using a thermogravimetric analyzer (TGA Q500, TA Instruments, New Castle, Delaware). During TPO, the catalyst was preheated to 373 K (heating rate 10 K min^{-1}) for 30 min under N_2 (100 ml min^{-1}) atmosphere. Thereafter, the temperature was increased from 373 to 1023 K (10 K min^{-1} ramping rate) under 3 N_2:1 O_2 flow. Under N_2 atmosphere, the sample was cooled to ambient temperature and was isothermally heated. Isothermal heating of the sample was carried out for 30 min and the sample had to be cooled with N_2 to reach ambient temperature. Micromeritics AutoChem II-2920 chemisorption system was utilized to determine both catalyst and support acidic properties. Before each measurement, approximately 0.1 g of the sample was pretreated at 773 K for 1 h at 50 ml min^{-1} under He flow to eliminate moisture and physisorbed compounds. The sample was cooled to 423 K under inert atmosphere after reduction in situ. Thereafter, adsorption was performed for 30 min at the same temperature in 50 ml min^{-1} of 10 %H_2/Ar. The NH_3 molecules in the gas phase were removed by purging with He gas for 30 min at 423 K after 1 h of adsorption using 5 % NH_3 in He balance. As part of the purging process at the same temperature with He gas for 30 min, NH_3 molecules were removed from the gas phase by heating at 1073 K (heating rate 10 K min^{-1}) for 10 min. Thermal conductivity detectors (TCD) were used to measure the quantity of desorbed NH_3 gas entering the U-tube from the outlet.

2.3. Catalytic activity test

A quartz tube reactor having an outer diameter of 3/8 in. and length of 17 in. was used to conduct OEDR experiments. This reactor was placed vertically within a split tubular furnace (LT furnace) during the experiments with stoichiometrically set to 3:1:1 for C_2H_5OH: CO_2:O_2 and temperatures between 773 and 973 K under atmospheric pressure. OEDR was performed on the catalyst by reducing it to 973 K with 50 % H_2/N_2 (60 ml min^{-1}) with heating at a rate of 10 Kmin^{-1} for 2 h before the reaction. The quartz tube reactor was filled with approximately 0.1 g_{cat} of the catalyst surrounded by a layer of quartz wool. In this experiment, KellyMed KL602 syringe pump (Beijing, China) and Alicat mass flow controller (Tucson, Arizona) were employed to ensure that ethanol and gas (viz, CO_2, O_2 reactant and N_2 diluent) were accurately fed to the top of the reactor. The gas hourly space velocity (GHSV) was calculated as 42 L g_{cat}^{-1} h^{-1} for each reaction. To obtain the intrinsic catalytic activity, high GHSV, small catalyst loadings, and tiny particle sizes were selected in order to ensure negligible mass and heat transfer resistances. The detailed calculation is included in the supplementary information for avoiding the mass and heat transfer intrusions. To maintain the 70 ml min^{-1} flow rate, N_2 was used as a tie component. As part of the analysis, a gas chromatograph (GC) from the Agilent 6890 Series (Agilent, Santa Clara, California) fitted with FID and TCD detectors to determine the composition of the gaseous effluent. The carbon balance is calculated by dividing the total moles of carbon in the products with the total moles of carbon reacted. The carbon mass balance was carried out for each run of the reaction, and it was greater than 91.3 %−98.8 %, confirming their remarkable resilience toward coke deposition during the OEDR.

3. Results and discussion

3.1. Physicochemical properties of the catalyst

The γ-Al_2O_3 support and 10 %Co/Al_2O_3 catalyst were examined for their textural characteristics, such as BET surface area, average pore volume, and pore diameter. It was observed that the γ-Al_2O_3 support had a relatively BET area of 175.2 m^2 g^{-1}, an average pore volume of 0.46 cm^3 g^{-1}, and a pore diameter of 10.7 nm. However, the surface area, pore-volume, and pore size of the 10 %Co/Al_2O_3 catalyst were smaller having values of 143.1 m^2 g^{-1}, 0.36 cm^3 g^{-1} and 10.6 nm, respectively. This could possibly be due to the introduction of Co oxides onto the γ-Al_2O_3 support surface.

Fig. 1 displays the comparison of fresh and spent XRD profiles of 10 %Co/Al_2O_3 catalyst and the calcined γ-Al_2O_3 support. The Joint Committee on Powder Diffraction Standards database was utilized to obtain a qualitative interpretation of the crystalline phase present in all specimens [22]. The γ-Al_2O_3 phase peaks at 2θ of 18.92°, 32.88°, 37.10°, 45.61°, and 67.17° was detected on fresh 10 %Co/Al_2O_3 catalyst (JCPDS card number: 04–0858) see Fig. 1(a). Furthermore, the spinel $CoAl_2O_4$

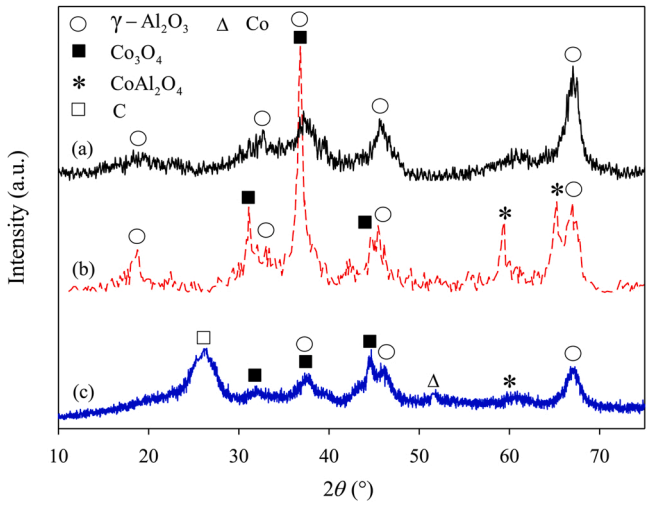

Fig. 1. XRD profiles of (a) gamma-Al_2O_3 support, (b) fresh 10 %Co/Al_2O_3 and (c) spent 10 %Co/Al_2O_3 catalyst at $P_{CO_2} = P_{O_2} = 5$ kPa,$P_{C_2H_5OH} = 15$ kPa and $T = 973$ K.

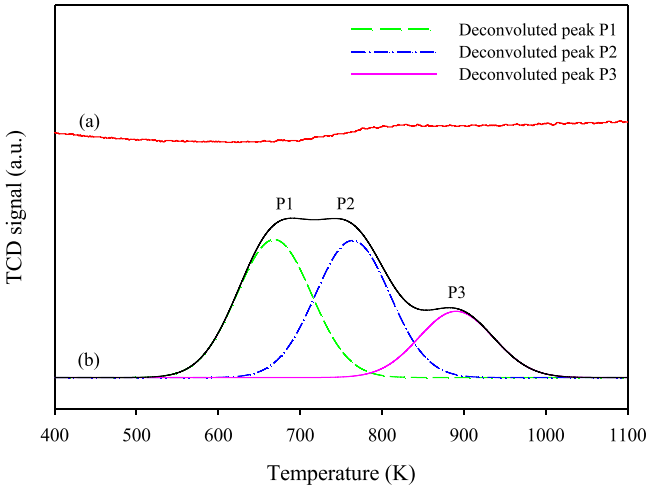

Fig. 2. Profiles of H_2-TPR on (a) gamma-Al_2O_3 support and (b) 10 % Co/Al_2O_3 catalyst ramped up at a rate of 10 K min^{-1}.

phase was observed at 2θ of 59.51° and 65.38° (JCPDS card number: 82–2246) over 10 %Co/Al_2O_3 catalyst. This was due to strong metal support interaction between Al_2O_3 and CoO, resulting in the formation of $CoAl_2O_4$ (see Fig. 1(b) and (c)) [23]. However, $CoAl_2O_4$ form was also observed on spent specimens (see Fig. 1(c)). As a result, it would be expected that the low peak intensity and absence of $2\theta = 65.38°$ would indicate that the lower amount of $CoAl_2O_4$ phase on the spent catalyst than the fresh catalyst could be due to the reduction of H_2 to Co^0 during activation. The XRD patterns of spent 10 %Co/Al_2O_3 catalyst after the OEDR at P_{CO_2}=P_{O_2}= 5 kPa,$P_{C_2H_5OH}$= 15, and 973 K is shown in Fig. 1(c). In both fresh and spent samples, Co_3O_4 phase was detected at 2θ of 31.45°, 37.10°, and 44.79° (JCPDS card number: 74–2120) see Fig. 1(b) and (c). However, the presence of the Co_3O_4 phase on the spent catalyst indicates that the Co^0 metallic phase was unavoidably re-oxidized during the OEDR process due to the catalyst being sufficiently reduced in H_2. Based on a diffractogram of the spent catalyst, the first broad peak centered around 2θ of 26.38° can be attributed to graphitic carbon (JCPDS card number: 75–0444) that is likely to have formed during the decomposition of ethanol and cracking of CH_4 intermediate at a high temperature [24]. Additionally, a new peak was observed on spent catalyst at 2θ of 51.50° (JCPDS card number: 15–0806) can be attributed to the Co phase [25,26]. Consequently, the stability of the catalytic performance can be attributed to the maintenance of the active metal phase after the OEDR process.

The H_2-TPR method was performed to investigate the reducibility of catalyst and support. According to Fig. 2(a), the H_2-TPR analysis of calcined γ-Al_2O_3 did not indicate any reduction peaks and it was stable and did not reduce in response to H_2. Furthermore, three significant peaks (P1, P2, and P3) were observed on 10 %Co/Al_2O_3 catalyst surface (Fig. 2(b)). P1 at temperatures between 458 and 720 K was due to the reduction of Co_3O_4 into intermediate CoO (cf. Eq. 2), while P2 at temperatures between 743 and 765 K corresponds to the reduction of CoO into metallic Co^0 (cf. Eq. 3) [27]. Moreover, another shoulder peak (P3) was observed at temperatures between 766 and 1014 K. This is attributed to the reduction of the spinel $CoAl_2O_4$ phase into the metallic Co^0 phase [28] (see Eq. 4).

$$Co_3O_4 + H_2 \rightarrow 3CoO + H_2O \quad (2)$$

$$CoO + H_2 \rightarrow Co + H_2O \quad (3)$$

$$CoAl_2O_4 + H_2 \rightarrow Co + Al_2O_3 + H_2O \quad (4)$$

In addition, Papageridis et al. [29] have also revealed that, due to high calcination temperatures, Co^{2+} ions migrate into the lattice of Al_2O_3 support and persist in tetrahedral positions in spinel $CoAl_2O_4$. As a result, CoO and Al_2O_3 interact strongly in $CoAl_2O_4$ species, which can produce a strong resistance to H_2 reduction.

Fig. 3 shows a measurement of the NH_3-TPD over γ-Al_2O_3 support and 10 %Co/Al_2O_3 catalyst. The γ-Al_2O_3 support and 10 %Co/Al_2O_3 catalyst exhibit weak, medium, and strong acid sites for different desorption temperatures ranging from 423 to 570 K, 571–710 K, and 721–1026 K, respectively [30,31]. Consequently, the strong acid sites possess a higher NH_3 desorption temperature than 713 K and is likely that they correspond to Brønsted acid sites. However, while the weak and medium acid sites possess a lower NH_3 desorption temperature, indicating the presence of Lewis and/or Brønsted acids sites [32]. According to Fig. 3, the γ-Al_2O_3 support contains three different acid centres, resulting in an overall NH_3 uptake of 4.77 mmol NH_3 g_{cat}^{-1}. Adding Co metal to γ-Al_2O_3 significantly improved the NH_3 uptake from 4.77 to 6.89 mmol NH_3 g_{cat}^{-1} (about 44.4 %). Based on this observation, it is possible that an extra acid site is formed at the interface between the Co metal and γ-Al_2O_3 support. Cheng et al. [33] reported that the adding Co to the calcined support increased acid site concentration and increased strong acid site concentration. According to this observation, some weak acid sites were replaced during thermal activation by impregnating Co species, resulting in strong acid sites. Thus, the catalytically active site may be protonated and likely located at the interface

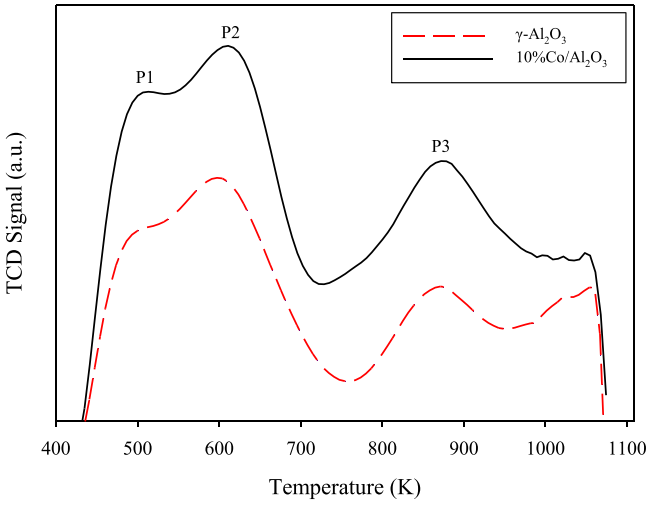

Fig. 3. NH_3-TPD profiles of Al_2O_3 support and 10 %Co/Al_2O_3 catalyst.

between the metal and alumina support.

In terms of carbon formation on a surface, it is well known that the acidity of the surface is a significant factor, whether the surface is the catalyst or the support. The formation of carbon is accelerated by positively charged acidic sites on a surface due to acidic sites catalyzing the cracking reaction. Gamma alumina is generally used as a support material during the reforming process, and its acidic properties facilitate carbon formation [34,35].

3.2. Oxidative ethanol dry reforming evaluation

This study examined the effect of reaction temperature over 10 %Co/Al_2O_3 catalyst with stoichiometric amounts of P_{CO_2}=P_{O_2}= 5 kPa, and$P_{C_2H_5OH}$= 15 kPa. The study was conducted within a temperature range of 773 and 973 K under atmospheric pressure. As illustrated in Fig. 4, temperature increase from 773 to 973 K resulted in increased conversions of C_2H_5OH and CO_2 by 22.5–93.6 % and 16.9–52.8 %, respectively. This observation can be attributed to the ethanol decomposition reaction (see Eq. (5)) [36].

$$C_2H_5OH \rightarrow CO + H_2 + CH_4 \quad (\Delta H^0_{298K} = 50.1\ kJmol^{-1}) \tag{5}$$

The reason for the enhanced performance of C_2H_5OH conversion rather than CO_2 conversion is the presence of side reactions with reasonable decomposition of ethanol and dehydrogenation. The significant conversion of C_2H_5OH over CO_2 was due to the numerous dehydrogenation and ethanol decomposition side reactions [37]. Furthermore, the addition of O_2 during the reforming reaction suppresses carbon formation and decreases the required heat, resulting in an exothermic reaction [38].

Fig. 5 illustrates the yields of CO, H_2 and CH_4 as a function of temperature at P_{CO_2} = P_{O_2} = 5 kPa, and$P_{C_2H_5OH}$ = 15 kPa. With an increase in temperature from 773 K to 973 K, the yield of both products (H_2 and CO) increased from 16.0 % to 68.1 % and 13.5–58.3 %, respectively. Increasing the temperature resulted in an increase in both H_2 and CO, which is consistent with the endothermic nature of Eq. (1). On the other hand, CH_4 yield also increased with rising reaction temperature (see Fig. 5). This indicates that during the C_2H_5OH decomposition (see Eq. (5)), CH_4 production rate was higher than the CH_4 reforming rate (reforming of CH_4 by CO_2 to produce syngas). Besides, this may indicate the successful conversion of ethanol into syngas [39]. As Bartholomew previously reported, the increase in CH_4 yield with reaction temperature may be due to lower carbon deposition (methane dehydrogenation) [40]. Moreover, O_2 as a reactant decreased the amount of carbon deposition during the OEDR reaction while improving the stability of the catalytic reaction for a long period of time.

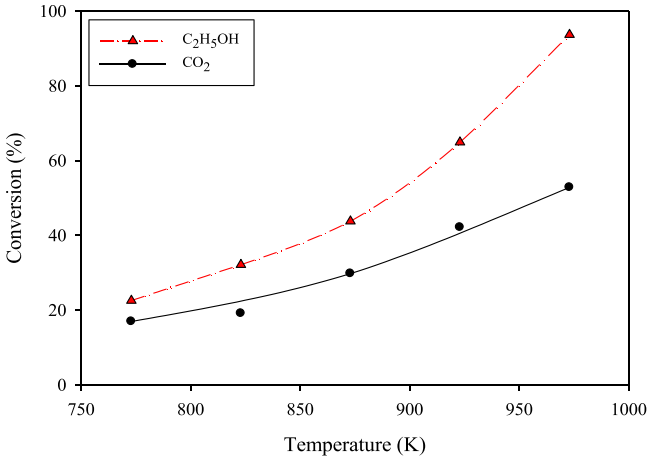

Fig. 4. Conversion of C_2H_5OH and CO_2 on 10 % Co/Al_2O_3 catalyst as a function of temperature at P_{CO_2} = P_{O_2} = 5 kPa and $P_{C_2H_5OH}$ = 15 kPa.

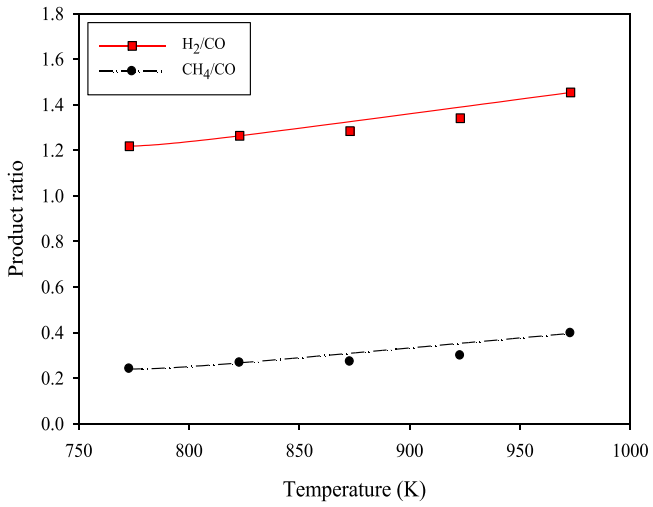

Fig. 5. Product yields over 10 % Co/Al_2O_3 catalyst as a function of temperature at P_{CO_2}= P_{O_2}= 5 kPa and $P_{C_2H_5OH}$ = 15 kPa.

The CH_4/CO and H_2/CO ratios are determined by varying the reaction temperature at P_{CO_2}= P_{O_2}= 5 kPa and = 15 kPa in Fig. 6. Increasing reaction temperature resulted in a linear increase of H_2/CO ratio from 1.2 to 1.5, indicating an improved C_2H_5OH dehydrogenation reaction [41]. As the reaction temperature increased, CH_4/CO ratio improved. It indicates that the rate of dry reforming of CH_4 was lower than the rate of C_2H_5OH decomposition. Alongside, the preferred CO/H_2 ratio is less than 2 and can be used as feedstocks in Fischer-Tropsch synthesis to produce green fuels [42].

Table 1 shows the summary of the evaluation of the 10 %Co/Al_2O_3 catalyst for OEDR, as well as other catalysts recently used in the oxidative steam reforming (OSR) reaction. Based on the results shown in Table 1, the 10 %Co/Al_2O_3 catalyst exhibited relatively comparable conversion of C_2H_5OH and H_2 selectivity during the OEDR runs when compared with other Co-based and noble-based catalysts in the literature. Even though the 10 %Co/Al_2O_3 catalyst in this study has a slightly lower activity than noble metal catalysts, from a practical and economic standpoint, it would be a useful catalyst for large-scale syngas production via OEDR.

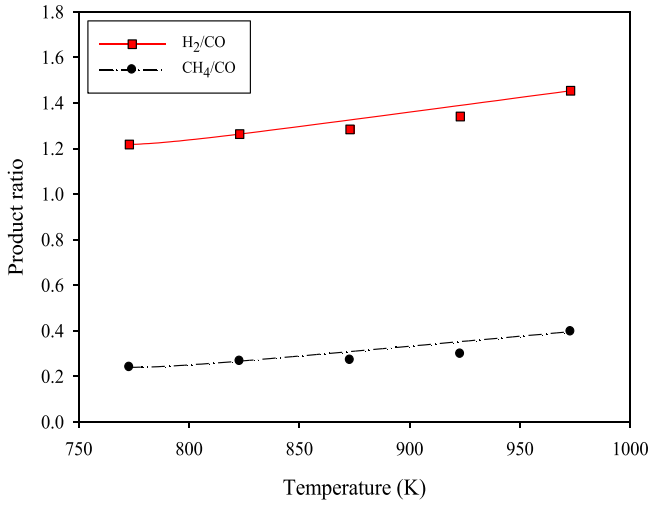

Fig. 6. Product ratio over 10 % Co/Al_2O_3 catalyst as a function of temperature at P_{CO_2}= P_{O_2}= 5 kPa and $P_{C_2H_5OH}$ = 15 kPa.

Table 1
Summary of oxidative dry reforming performance on different catalysts reported in literature.

Catalyst	Reaction condition				Conversion EtOH (%)	Selectivity H_2 (%)	Ref.
	Temperature (K)	Gas hourly spece velocity	Time-on-stream (h)	Molar ratio H_2O/EtOH/O_2			
Ni/γ-Al_2O_3	923	[a]n.m.	2.8	1.5/1/0.2	99	63	[43]
15Ni/CeZrAl	973	100.000 h^{-1}	6.2	3/1/0.5	99.9	65	[44]
5 %Rh/Al_2O_3	973	n.m.	140	1.6/1/0.68	95	30	[45]
8 %Co/SiO_2	673	5.000 h^{-1}	15	6/1/0.5	80	45	[20]
5 %NiRh/CeO_2	623	24.379 h^{-1}	70	4–1–0.4	94	52	[46]
6 %Co/γ-Al_2O_3	773	n.m.	1.5	3/1/0.5	97	40	[47]
10 %Co/CeO_2	773	n.m.	50	3/1/0.5	100	58	[18]
30 %Ni/CeO_2-ZrO_2	923	n.m.	15	8/1/0.5	100	75	[48]
9 %Ir/La_2O_3	873	50.000 h^{-1}	100	3/1/0.8	100	65	[49]
2 %Ir/CeO_2	773	6.000 ml gcat h^{-1}	60	1.8/1/0.6	100	57	[50]
10 %Co/Al_2O_3	773	42 L g_{cat} h^{-1}	8	[b]1/3/1	22.5	45	This study
	823	42 L g_{cat} h^{-1}	8	[b]1/3/1	32.1	47	This study
	873	42 L g_{cat} h^{-1}	8	[b]1/3/1	43.7	49	This study
	923	42 L g_{cat} h^{-1}	8	[b]1/3/1	64.9	50	This study
	973	42 L g_{cat} h^{-1}	8	[b]1/3/1	93.6	52	This study

[a] n.m.: not mentioned.
[b] Indicating the ratio of CO_2/C_2H_5OH/O_2 during the OEDR.

3.3. Carbon formation and catalyst deactivation

TPO measurements were used to determine the amount of carbon deposition on the surface of the spent 10 %Co/Al_2O_3 catalyst. Fig. 7 shows the TPO results for the weight percentage of the spent sample. The spent 10 %Co/Al_2O_3 catalyst deposited the least amount of carbon (28,92 %) at 973 K. Nevertheless, the reaction temperature decreased from 973 to 773 K, and the amount of carbon deposition improved by 41.48 %. This demonstrates quicker deposition of carbon on the catalyst surface. As shown in Figs. 4 and 7, the trend of carbon weight vs. temperature curve is opposite to that of CO_2 and C_2H_5OH conversions, further indicating that the catalytic activity improved via the oxidization of carbonaceous deposition. On the other hand, XRD analysis also showed that graphitic carbon was present on the surface of the spent catalyst (see Fig. 1(c)). Ruckenstein and Wang also reported that the stability of Co/γ-Al_2O_3 catalysts with several Co loadings and calcination temperature (6 wt. % for Tc =500 °C and 9 wt. % for Tc =1000 °C) exhibited stable activity. However, catalysts with high Co loadings (above 12 wt. %) accumulated significant amounts of carbon during reforming and demonstrated deactivation [51]. Thus, the reduction of carbon deposited on the catalyst surface resulted in a higher conversion of C_2H_5OH and CO_2.

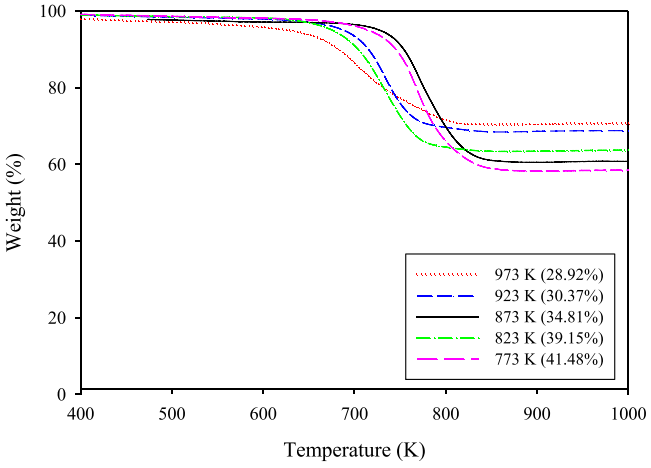

Fig. 7. Weight percentage profiles of spent 10 %Co/Al_2O_3 catalyst from 773 to 973 K with a 10 K min^{-1} heating rate.

4. Conclusions

The present study describes the OEDR for syngas production over Co/Al_2O_3 catalyst at various reaction temperatures. The catalyst design consists of 10 wt % Co and γ-Al_2O_3 support with a high specific surface area, which can prevent the sintering impact. OEDR allows the active metal phase of the catalyst to be maintained during the catalytic process, which contributes to a stable catalytic performance. The interaction between CoO and Al_2O_3 can produce $CoAl_2O_4$ species, and these compounds exhibit strong resistance to H_2 reduction. The level of NH_3 uptake was increased significantly from 4.77 to 6.89 mmol NH_3 g_{cat}^{-1}, resulting in the formation of extra acid sites at the interface of the Co metal and γ-Al_2O_3 support. The catalyst displays high performance for oxidative ethanol dry reforming to generate synthesis gas. Thus, it is a suitable candidate to be used as a fuel for internal combustion engines and as a chemical feedstock for the production of ammonia and methanol. According to tests conducted under various reaction temperatures, the conversion of C_2H_5OH and CO_2 increased with an increase in reaction temperature and decreased with a decrease in reaction temperature. Further, the addition of oxygen to the feed gas enhances the production of H_2, CO, and CH_4 while at the same time limiting the accumulation of carbon.

Declaration of Competing Interest

The authors declare that they have no known competing financial interests or personal relationships that could have appeared to influence the work reported in this paper.

Data Availability

Data will be made available on request.

Acknowledgments

The authors acknowledge the financial support from the Universiti Malaysia Pahang (UMP) Research Grant Scheme (RDU130376). Fahim Fayaz would like to thank Dr. Dai-Viet N. Vo for his invaluable guidance and support during the research work. Fahim Fayaz is also grateful for the funds received from the Institute of International Education's Scholar Rescue Fund (IIE-SRF) and the Finnish National Agency for Education (EDUFI) for supporting his postdoctoral fellowship at

Tampere University.

Appendix A. Supporting information

Supplementary data associated with this article can be found in the online version at doi:10.1016/j.mtcomm.2023.105671.

References

[1] L. Ai, H. Fan, CTAB-melamine molecular crystals as precursor for synthesis of layered carbon nitride porous nanostructures with enhanced photocatalytic activity for hydrogen production, Mater. Today Commun. 29 (2021), 102780, https://doi.org/10.1016/j.mtcomm.2021.102780.

[2] B. Narindri, R. Winayu, B. Li, H. Chu, Fe_2O_3/TiO_2 oxygen carrier for chemical looping combustion of CO, H_2, and CH_4 in a fluidized bed reactor, Mater. Today Commun. 32 (2022), 104026, https://doi.org/10.1016/j.mtcomm.2022.104026.

[3] B. Abdullah, N. Azeanni, A. Ghani, D.N. Vo, Recent advances in dry reforming of methane over Ni-based catalysts, J. Clean. Prod. 162 (2017) 170–185, https://doi.org/10.1016/j.jclepro.2017.05.176.

[4] K. Saravanan, H. Ham, N. Tsubaki, J.W. Bae, Recent progress for direct synthesis of dimethyl ether from syngas on the heterogeneous bifunctional hybrid catalysts, Appl. Catal. B: Environ. 217 (2017) 494–522, https://doi.org/10.1016/j.apcatb.2017.05.085.

[5] A.H. Elbadawi, L. Ge, Z. Li, S. Liu, S. Wang, Catalytic partial oxidation of methane to syngas: review of perovskite catalysts and membrane reactors, Catal. Rev. - Sci. Eng. 63 (2021) 1–67, https://doi.org/10.1080/01614940.2020.1743420.

[6] X. Liu, H. Chen, J. Yuan, X. Li, J. Yu, Evaluation and screening of metal-organic frameworks for the adsorption and separation of methane and hydrogen, Mater. Today Commun. 33 (2022), 104602, https://doi.org/10.1016/j.mtcomm.2022.104602.

[7] K. Świrk, M.E. Gálvez, M. Motak, T. Grzybek, M. Rønning, P. Da Costa, Dry reforming of methane over Zr- and Y-modified Ni/Mg/Al double-layered hydroxides, Catal. Commun. 117 (2018) 26–32, https://doi.org/10.1016/j.catcom.2018.08.024.

[8] C. Jiménez-González, M. Gil-Calvo, B. de Rivas, J.R. González-Velasco, J. I. Gutiérrez-Ortiz, A. RubénLópez-Fonseca, Oxidative steam reforming and steam reforming of methane, isooctane, and n-tetradecane over an alumina supported spinel-derived nickel catalyst, Ind. Eng. Chem. Res. 55 (2016) 3920–3929, https://doi.org/10.1021/acs.iecr.6b00461.

[9] A.S. Russel, Microkinetic and sensitivity analysis of oxidative dry reforming of methane on Ni–Co catalyst using a reaction mechanism based on Ni, React. Chem. Eng. 6 (2021) 2104–2113, https://doi.org/10.1039/d1re00086a.

[10] F. Mamusi, D. Farmanzadeh, Mechanism of ethanol steam reforming on $B_{12}N_{12}$ and Al_{12} N_{12} nano-cages: a theoretical study, Mater. Today Commun. 30 (2022), 103014, https://doi.org/10.1016/j.mtcomm.2021.103014.

[11] F. Fayaz, N.T.A. Nga, T.L.M. Pham, H.T. Danh, B. Abdullah, H.D. Setiabudi, D.-V. N. Vo, Hydrogen production from ethanol dry reforming over lanthania-promoted Co/Al_2O_3 catalyst, IIUM Eng. J. 19 (2018), https://doi.org/10.31436/iiumej.v19i1.813.

[12] T. Mondal, K.K. Pant, A.K. Dalai, Catalytic oxidative steam reforming of bio-ethanol for hydrogen production over Rh promoted Ni/CeO_2-ZrO_2 catalyst, Int. J. Hydrog. Energy 40 (2015) 2529–2544, https://doi.org/10.1016/j.ijhydene.2014.12.070.

[13] A. Haryanto, S. Fernando, N. Murali, S. Adhikari, Current status of hydrogen production techniques by steam reforming of ethanol: a review, Energ. Fuel. 19 (2005) 2098–2106.

[14] M. Ni, D.Y.C. Leung, M.K.H. Leung, A review on reforming bio-ethanol for hydrogen production, Int. J. Hydrog. Energy 32 (2007) 3238–3247, https://doi.org/10.1016/j.ijhydene.2007.04.038.

[15] M. Mohammadi, G.D. Najafpour, H. Younesi, P. Lahijani, M.H. Uzir, A. R. Mohamed, Bioconversion of synthesis gas to second generation biofuels: a review, Renew. Sustain. Energy Rev. 15 (2011) 4255–4273, https://doi.org/10.1016/j.rser.2011.07.124.

[16] O. Omoregbe, H.T. Danh, C. Nguyen-Huy, H.D. Setiabudi, S.Z. Abidin, Q. D. Truong, D.-V.N. Vo, Syngas production from methane dry reforming over Ni/SBA-15 catalyst: effect of operating parameters, Int. J. Hydrog. Energy 42 (2017) 11283–11294, https://doi.org/10.1016/j.ijhydene.2017.03.146.

[17] O. Akdim, W. Cai, V. Fierro, H. Provendier, A.V. Veen, W. Shen, C. Mirodatos, Oxidative steam reforming of ethanol over Ni–Cu/SiO_2, Rh/Al_2O_3 and Ir/CeO_2: Effect of metal and support on reaction mechanism, Top. Catal. 51 (2008) 22–38, https://doi.org/10.1007/s11244-008-9122-z.

[18] S.M. De Lima, M. Adriana, O.O. Lídia, U.M. Graham, G. Jacobs, B.H. Davis, L. V. Mattos, F.B. Noronha, Study of catalyst deactivation and reaction mechanism of steam reforming, partial oxidation, and oxidative steam reforming of ethanol over Co/CeO_2 catalyst, J. Catal. 268 (2009) 268–281, https://doi.org/10.1016/j.jcat.2009.09.025.

[19] L.M. Andre, L.V. Mattos, J.P. Den Breejen, J.H. Bitter, K.P. De Jong, F.B. Noronha, Oxidative steam reforming of ethanol over carbon nanofiber supported Co catalysts, Catal. Today 164 (2011) 262–267, https://doi.org/10.1016/j.cattod.2010.11.013.

[20] E.B. Pereira, N. Homs, S. Martí, J.L.G. Fierro, P. Ramírez, D. Piscina, Oxidative steam-reforming of ethanol over Co/SiO_2, Co – Rh/SiO_2 and Co – Ru/SiO_2 catalysts: catalytic behavior and deactivation/ regeneration processes, J. Catal. 257 (2008) 206–214, https://doi.org/10.1016/j.jcat.2008.05.001.

[21] M. Farid, F. Sukri, M. Khavarian, Effect of cobalt loading on suppression of carbon formation in carbon dioxide reforming of methane over Co/MgO catalyst, Res. Chem. Intermed. 44 (2018) 2585–2605, https://doi.org/10.1007/s11164-017-3248-1.

[22] JCPDS Powder Diffraction File, International Centre for Diffraction Data. Swarthmore, PA, (2000).

[23] L. Ji, J. Lin, H.C. Zeng, Metal-support interactions in Co/Al_2O_3 catalysts: a comparative study on reactivity of support, J. Phys. Chem. B 104 (2000) 1783–1790, https://doi.org/Doi 10.1021/Jp993400l.

[24] S.Y. Foo, C.K. Cheng, T.-H. Nguyen, E.M. Kennedy, B.Z. Dlugogorski, A.A. Adesina, Carbon deposition and gasification kinetics of used lanthanide-promoted Co-Ni/Al_2O_3 catalysts from CH_4 dry reforming, Catal. Commun. 26 (2012) 183–188, https://doi.org/10.1016/j.catcom.2012.06.003.

[25] Z.-Y. Wu, P. Chen, Q.-S. Wu, L.-F. Yang, Z. Pan, Q. Wang, Co/Co_3O_4/C-N, a novel nanostructure and excellent catalytic system for the oxygen reduction reaction, Nano Energy 8 (2014) 118–125, https://doi.org/10.1016/j.nanoen.2014.05.019.

[26] D. Homsi, S. Aouad, C. Gennequin, A. Aboukaïs, E. Abi-Aad, A highly reactive and stable Ru/Co_6-$xMgxAl_2$ catalyst for hydrogen production via methane steam reforming, Int. J. Hydrog. Energy 39 (2014) 10101–10107, https://doi.org/10.1016/j.ijhydene.2014.04.151.

[27] E.B. Pereira, P.R. de la Piscina, S. Martí, N. Homs, H_2 production by oxidative steam reforming of ethanol over K promoted $Co-Rh/CeO_2$-ZrO_2 catalysts, Energy Environ. Sci. 3 (2010) 486–492, https://doi.org/10.1039/b924624j.

[28] C.G. Cooper, T.H. Nguyen, Y.J. Lee, K.M. Hardiman, T. Safinski, F.P. Lucien, A. A. Adesina, Alumina-supported cobalt-molybdenum catalyst for slurry phase Fischer-Tropsch synthesis, Catal. Today 131 (2008) 255–261, https://doi.org/10.1016/j.cattod.2007.10.056.

[29] K.N. Papageridis, G. Siakavelas, N.D. Charisiou, D.G. Avraam, L. Tzounis, K. Kousi, M.A. Goula, Comparative study of Ni, Co, Cu supported on γ-alumina catalysts for hydrogen production via the glycerol steam reforming reaction, Fuel Process. Technol. 152 (2016) 156–175, https://doi.org/10.1016/j.fuproc.2016.06.024.

[30] M. Firoozi, M. Baghalha, M. Asadi, The effect of micro and nano particle sizes of H-ZSM-5 on the selectivity of MTP reaction, Catal. Commun. 10 (2009) 1582–1585, https://doi.org/10.1016/j.catcom.2009.04.021.

[31] M.A.F. e Santos, I.P. Lôbo, R.S. da Cruz, Synthesis and characterization of novel ZrO_2-SiO_2 mixed oxides, Mater. Res. 17 (2014) 700–707, https://doi.org/10.1590/S1516-14392014005000046.

[32] W. Zhang, E.C. Burckle, P.G. Smirniotis, Characterization of the acidity of ultrastable Y, mordenite, and ZSM-12 via NH_3-stepwise temperature programmed desorption and Fourier transform infrared spectroscopy, Microporous Mesoporous Mater. 33 (1999) 173–185, https://doi.org/10.1016/S1387-1811(99)00136-5.

[33] C.K. Cheng, S.Y. Foo, A.A. Adesina, H_2-rich synthesis gas production over Co/Al_2O_3 catalyst via glycerol steam reforming, Catal. Commun. 12 (2010) 292–298, https://doi.org/10.1016/j.catcom.2010.09.018.

[34] L.M. Andre, L.V. Mattos, J.P. Den Breejen, J.H. Bitter, K.P. De Jong, F.B. Noronha, Oxidative steam reforming of ethanol over carbon nanofiber supported Co catalysts, Catal. Today 164 (2011) 262–267, https://doi.org/10.1016/j.cattod.2010.11.013.

[35] Y. Jiao, H. Zhang, S. Li, C. Guo, P. Yao, J. Wang, Impact of acidity in ZrO_2 -TiO_2 -Al_2O_3 composite oxides on the catalytic activity and coking behaviors during n-decane cracking, Fuel 233 (2018) 724–731, https://doi.org/10.1016/j.fuel.2018.06.011.

[36] T.A. Maia, J.M. Assaf, E.M. Assaf, Study of Co/CeO_2-γ-Al_2O_3 catalysts for steam and oxidative reforming of ethanol for hydrogen production, Fuel Process. Technol. 128 (2014) 134–145, https://doi.org/10.1016/j.fuproc.2014.07.009.

[37] M.B. Bahari, N.H.H. Phuc, B. Abdullah, F. Alenazey, D.-V.N. Vo, Ethanol dry reforming for syngas production over Ce-promoted Ni/Al_2O_3 catalyst, J. Environ. Chem. Eng. 4 (2016) 4830–4838, https://doi.org/10.1016/j.jece.2016.01.038.

[38] S.Y. Foo, C.K. Cheng, T.-H. Nguyen, A. a Adesina, Kinetic study of methane CO_2 reforming on Co–Ni/Al_2O_3 and Ce–Co–Ni/Al_2O_3 catalysts, Catal. Today 164 (2011) 221–226, https://doi.org/10.1016/j.cattod.2010.10.092.

[39] F. Fayaz, L.G. Bach, M.B. Bahari, T.D. Nguyen, K.B. Vu, R. Kanthasamy, C. Samart, C. Nguyen-Huy, D.-V.N. Vo, Stability evaluation of ethanol dry reforming on Lanthania-doped cobalt-based catalysts for hydrogen-rich syngas generation, Int. J. Energy Res. 43 (2019) 405–416, https://doi.org/10.1002/er.4274.

[40] C.H. Bartholomew, Mechanisms of catalyst deactivation, Appl. Catal. A: Gen. 212 (2001) 17–60, https://doi.org/10.1016/S0926-860X(00)00843-7.

[41] F. Fayaz, M.B. Bahari, T.L.M. Pham, C. Nguyen-Huy, H.D. Setiabudi, B. Abdullah, D.-V.N. Vo, Hydrogen-rich syngas production via ethanol dry reforming over rare-earth metal-promoted Co-based catalysts, Recent Adv. Biofuels Bioenergy Util. (2018) 177–204.

[42] D.-V.N. Vo, T.-H. Nguyen, E.M. Kennedy, B.Z. Dlugogorski, A.A. Adesina, Fischer-Tropsch synthesis: effect of promoter type on alumina-supported Mo carbide catalysts, Catal. Today 175 (2011) 450–459, https://doi.org/10.1016/j.cattod.2011.04.045.

[43] L. Pérez-Moreno, J. Soler, J. Herguido, M. Menéndez, Stable steam reforming of ethanol in a two-zone fluidized-bed reactor, Ind. Eng. Chem. Res. 51 (2011) 8840–8848, https://doi.org/10.1021/ie201968u.

[44] N. Srisiriwat, S. Therdthianwong, A. Therdthianwong, Oxidative steam reforming of ethanol over Ni/Al_2O_3 catalysts promoted by CeO_2, ZrO_2 and CeO_2-ZrO_2, Int. J. Hydrog. Energy 34 (2009) 2224–2234, https://doi.org/10.1016/j.ijhydene.2008.12.058.

[45] V. Fierro, O. Akdim, C. Mirodatos, On-board hydrogen production in a hybrid electric vehicle by bio-ethanol oxidative steam reforming over Ni and noble metal

based catalysts, Green. Chem. 5 (2003) 20–24, https://doi.org/10.1039/B208201M.
[46] J. Kugai, S. Velu, C. Song, Low-temperature reforming of ethanol over CeO_2 -supported Ni-Rh bimetallic catalysts for hydrogen production, Catal. Lett. 101 (2005) 255–264, https://doi.org/10.1007/s10562-005-4901-7.
[47] S. Andonova, C.N. De Ávila, K. Arishtirova, J.M.C. Bueno, S. Damyanova, Structure and redox properties of Co promoted Ni/Al_2O_3 catalysts for oxidative steam reforming of ethanol, Appl. Catal. B, Environ. 105 (2011) 346–360, https://doi.org/10.1016/j.apcatb.2011.04.029.
[48] P. Biswas, D. Kunzru, Oxidative steam reforming of ethanol over Ni/CeO_2-ZrO_2 catalyst, Chem. Eng. J. 136 (2008) 41–49, https://doi.org/10.1016/j.cej.2007.03.057.
[49] H. Chen, H. Yu, F. Peng, H. Wang, J. Yang, M. Pan, Efficient and stable oxidative steam reforming of ethanol for hydrogen production: effect of in situ dispersion of Ir over Ir/La_2O_3, J. Catal. 269 (2010) 281–290, https://doi.org/10.1016/j.jcat.2009.11.010.
[50] T. Hou, S. Zhang, T. Xu, W. Cai, Hydrogen production from oxidative steam reforming of ethanol over Ir/CeO_2 catalysts in a micro-channel reactor, Chem. Eng. J. 255 (2014) 149–155, https://doi.org/10.1016/j.cej.2014.06.046.
[51] E. Ruckenstein, H.Y. Wang, Carbon deposition and catalytic deactivation during CO_2 reforming of CH_4 over Co/γ-Al_2O_3 catalysts, J. Catal. 205 (2002) 289–293, https://doi.org/10.1006/jcat.2001.3458.